Numerical investigation of two-dimensional projections of random fractal aggregates

Rémi Jullien and Romain Thouy
Laboratoire de Science des Matériaux Vitreux, Université Montpellier II, Place Eugène Bataillon. F-34095 Montpellier Cedex 5, France

Françoise Ehrburger-Dolle
Centre de Recherches sur la Physico-Chimie des Surfaces Solides, Centre National de la Recherche Scientifique, 24 Avenue du Président Kennedy, F-68200 Mulhouse, France

(Received 16 May 1994)

Three-dimensional random fractal aggregates of variable fractal dimension D ranging from 1 to 2.5 are built on a cubic lattice using a hierarchical computer algorithm. The fractal dimensions of the surface D_s and the perimeter D_p of their two-dimensional projections have been computed. From an extrapolation of finite size results for aggregates containing up to 8192 particles, it is found that D_s and D_p are both equal to D for $D < 2$ while $D_s = 2$ for $D > 2$. The numerical results are consistent with a nontrivial value of D_p, varying continuously with D, for $D > 2$.

PACS number(s): 61.43.Hv, 61.20.Ja, 61.16.−d

I. INTRODUCTION

The characterization of the morphology of finely divided solids made of aggregated particles by means of fractal geometry [1] led to a better understanding of the aggregation mechanism by which they are formed [2,3] and to their resulting physical and chemical properties [3,4]. Therefore, the experimental determination of the fractal dimension of mass fractal aggregates is of particular interest. Among the practical methods commonly used, one can distinguish quantitative analysis of digitalized electron micrographs [5–7] and small angle scattering neutron (x-ray or light) experiments [8–10]. Both methods encounter difficulties when they are applied to aggregates of fractal dimension larger than two since in that case the fractal dimension of their projection is bounded by two and the scattering cross section becomes cutoff dependent [11]. In this paper, we are concerned by the former method and we address this problem numerically by making use of a recently developed hierarchical cluster-cluster aggregation model [12] which allows one to build three-dimensional fractal aggregates on a cubic lattice with a tunable fractal dimension varying continuously from 1 to 2.5. We calculate some effective (size-dependent) fractal dimensions for the surface, $D_s(N)$, and the perimeter, $D_p(N)$, of the two-dimensional projection of such aggregates containing up to $N = 8192$ particles. These quantities exhibit strong size dependence for fractal dimensions close to two. When trying to extrapolate to the infinite size, they both converge to the actual fractal dimension D for $D < 2$. But, while $D_s(N)$ converges to the trivial value $D_s = 2$, $D_p(N)$ converges to a nontrivial, D-dependent value for $D > 2$.

II. THE VARIABLE-D CLUSTER-CLUSTER HIERARCHICAL ALGORITHM

We recall here the main principles of a recent algorithm which has been detailed elsewhere [12]. We use an iterative method which, starting from a collection of 2^n particles, builds, at iteration p, a collection of 2^{n-p} aggregates containing $N = 2^p$ particles each. The aggregates are built on a cubic lattice with nearest neighbor connection rules. An aggregate of the next generation, containing N particles, is obtained by sticking two aggregates of the previous generation, containing both $\frac{N}{2}$ particles, in a such a way that the distance Γ between their center of mass should satisfy at best the condition

$$\Gamma^2 = k^2 R^2_{\frac{N}{2}} + 1 \ , \tag{1}$$

where $R^2_{\frac{N}{2}}$ is the mean square radius of gyration of the two aggregates and k is related to the desired fractal dimension D by

$$k^2 = 4(4^{\frac{1}{D}} - 1) \ . \tag{2}$$

The final configuration is chosen at random among all the possibilities. Here we have considered version B of the model (using the terminology of Ref. [12]) in which some rotations of the clusters are allowed when trying to satisfy relation (1). Following previous works [12,13] one can calculate an effective, N-dependent fractal dimension, $D(N)$, by comparing the results of a given iteration with those of the previous one,

$$D(N) = \frac{\log 4}{\log(\langle R^2_N \rangle - \frac{1}{4}) - \log\langle R^2_{\frac{N}{2}} \rangle} \ , \tag{3}$$

where the brackets $\langle \cdots \rangle$ are averages over the collection of aggregates at a given iteration and where the term $\frac{1}{4}$ is introduced to eliminate "trivial" corrections to scaling [13,14]. In Ref. [12] it has been shown that for all D values smaller than $D_m = 2.5$, and as soon as N is larger than 16, $D(N)$ becomes almost size independent and is equal to D within less than 0.1%. In Fig. 1 we show typical two-dimensional projections of aggregates built with $D = 1.5, 2$, and 2.5, containing 8192 particles.

FIG. 1. Two-dimensional projections of typical aggregates of 8192 particles built with the variable-D cluster-cluster hierarchical procedure with $D = 1.5, 2, 2.5$. The scale has been chosen such that the vertical size is the same in all pictures.

III. NUMERICAL CHARACTERIZATION OF THE AGGREGATES PROJECTIONS

We have extended the above algorithm in order to calculate the geometrical characteristics of the two-dimensional projections of the aggregates. As soon as an aggregate is built, a storage is made for its projections on planes perpendicular to the x, y, and z directions of the cubic lattice. In doing so, we implicitly assume that our aggregates are purely isotropic so that these directions are equivalent to any other directions of space. This assumption, which is certainly wrong for deterministic aggregates, may be reasonably trusted here since our disordered fractal aggregates have been built with isotropic rules. A given projection is considered as a cluster on a square lattice, the particle of which are projections of one or more particles of the three-dimensional cluster. For each projection, one calculates the number of surface sites (occupied sites of the square lattice), N_s, and the number of perimeter sites, N_p, as being unoccupied sites nearest neighbors to occupied sites. Note that with such a definition the internal perimeter of holes is taken into account (it would have been difficult to exclude the holes contribution without slowing down the calculation). The quantities N_s and N_p are averaged over the three projections for each aggregate, over all the aggregates of one generation, and over several independent runs. Then, in coherence with formula (3), we have calculated size dependent fractal dimensions $D_s(N)$ and $D_p(N)$ by

$$D_s(N) = 2\frac{\log\langle N_s(N)\rangle - \log\langle N_s(\frac{N}{2})\rangle}{\log(\langle R_N^2\rangle - \frac{1}{4}) - \log\langle R_{\frac{N}{2}}^2\rangle}\ , \tag{4}$$

$$D_p(N) = 2\frac{\log\langle N_p(N)\rangle - \log\langle N_p(\frac{N}{2})\rangle}{\log(\langle R_N^2\rangle - \frac{1}{4}) - \log\langle R_{\frac{N}{2}}^2\rangle}\ , \tag{5}$$

As in the expression of $D(N)$ we have kept the subtraction by $\frac{1}{4}$ in the denominator, but here this trick has no reason to eliminate the leading corrections to scaling. If these quantities converge when N tends to infinity, their limits D_s and D_p are such that, in the asymptotic limit of an extremely large aggregate of radius of gyration R, one recovers the fractal scaling relations

$$N_s \sim R^{D_s}\ , \tag{6}$$

$$N_p \sim R^{D_p}\ . \tag{7}$$

In formulas (4) and (5) we have used the radius of gyration of the three-dimensional aggregates. There is no rigorous reason to do so and we might have used the radius of gyration of their projections instead. We have checked that in the two cases the results are very close and that, anyway, they lead to the same large-N extrap-

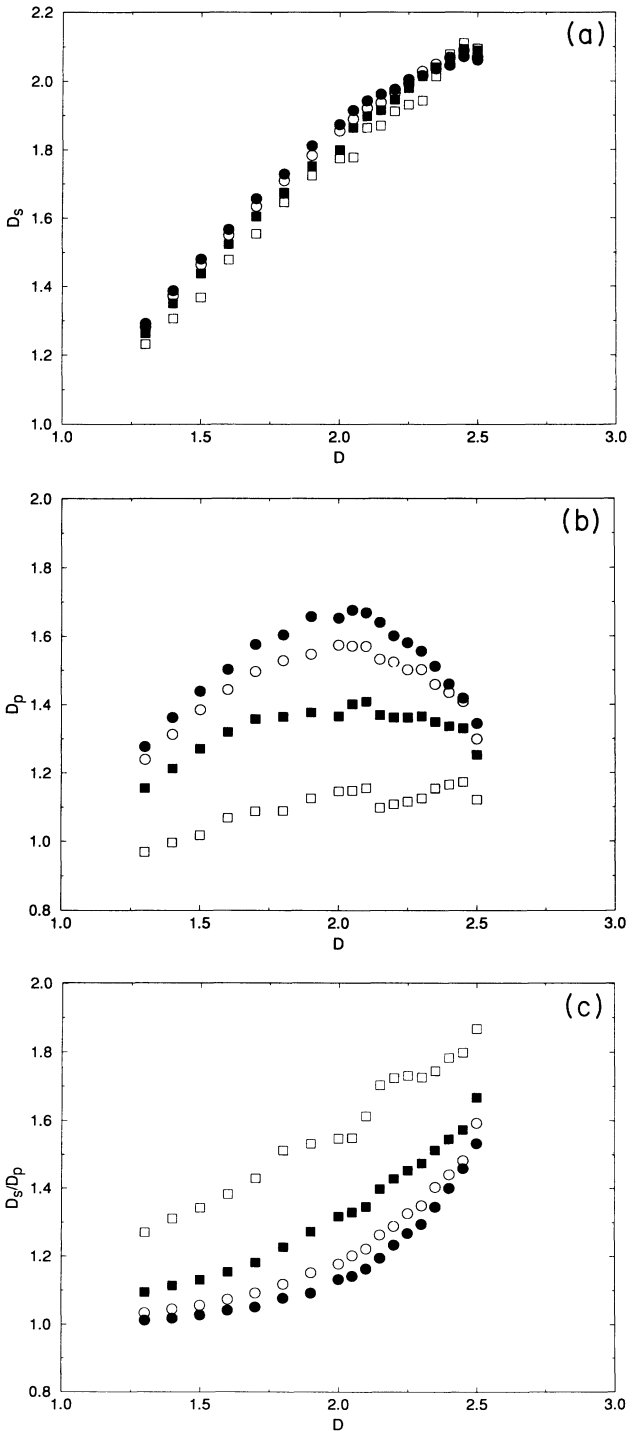

FIG. 2. Numerical results for the effective fractal dimensions $D_s(N)$ (a), $D_p(N)$ (b), and their ratio $\frac{D_s(N)}{D_p(N)}$ (c) as a function of D, for $N = 16$ (open squares), 128 (filled squares), 1024 (open circles), and 8192 (filled circles).

olated values within the numerical uncertainties.

We have considered fractal dimensions varying from 1.3 to 2.0 by intervals of 0.1, and from 2.0 to 2.5 by intervals of 0.05, up to size $N = 8192$, and 16 independent runs have been performed in each cases. In Figs. 2(a), 2(b), and 2(c), we give the numerical results for $D_s(N)$, $D_p(N)$, and for the ratio $\frac{D_s(N)}{D_p(N)}$, respectively, as a function of D, for some typical values of N ($N = 16, 128, 1024$, and 8192). In contrast with $D(N)$, both $D_s(N)$ and $D_p(N)$ are size dependent. It appears that finite size effects are stronger in the case of $D_p(N)$ and for fractal dimensions close to two. It can also be noticed that, in some range of parameters, it may happen that $D_p(N) < 1$ and that $D_s(N) > 2$. This is not forbidden because these N-dependent quantities are not true fractal dimensions (only their infinite-N extrapolations are).

IV. NUMERICAL EXTRAPOLATION PROCEDURE

Since we have no help from a theory, we will assume that, as $N \to \infty$, both $D_s(N)$ and $D_p(N)$ can be expressed as expansions of some unknown powers of $\frac{1}{N}$. For example, in the case of $D_s(N)$, such an expansion might be written as

$$D_s(N) = D_s + \sum_{i=1}^{\infty} A_s(i) N^{-\alpha_s(i)} , \tag{8}$$

where D_s is the true fractal dimension for the surface of the projection. In practice, we have truncated the sum to its first term, and we have tried to fit the data with

$$D_s(N) = D_s + A_s N^{-\alpha_s} , \tag{9}$$

where D_s, A_s, and α_s have been calculated to give the best fits (lowest standard deviation) for each D value. To avoid the strong systematic errors on very small sizes, we have not included the data for $N = 2, 4$, and 8 in the fits. This is more or less justified by the fact that $D(N)$ is found to be very close to the true fractal dimension as soon as N is greater or equal to 16. Therefore, it remains only ten points for each fit and it is clear, in view of the numerical uncertainties, that it is impossible to try to determine two terms of the sum (i.e., five unknown parameters). Some typical fits are shown in Fig. 3(a), where $D_s(N)$ has been plotted as a function of $(\frac{N}{16})^{-\alpha_s}$ (with the best α_s in each case) for D values smaller than 2.3. The procedure failed for $D > 2.3$ because $D_s(N)$ exhibits a nonmonotonic behavior. In the cases $D = 2.3$ and 2.5 we have arbitrarily taken $\alpha_s = 0.4$ to present the data for D_s in Fig. 3(a).

The same procedure has been used for $D_p(N)$ and for the ratio $\frac{D_s(N)}{D_p(N)}$ for which the following fits have been used:

$$D_p(N) = D_p + A_p N^{-\alpha_p} , \tag{10}$$

$$\frac{D_s(N)}{D_p(N)} = \frac{D_s}{D_p} + A_{sp} N^{-\alpha_{sp}} . \tag{11}$$

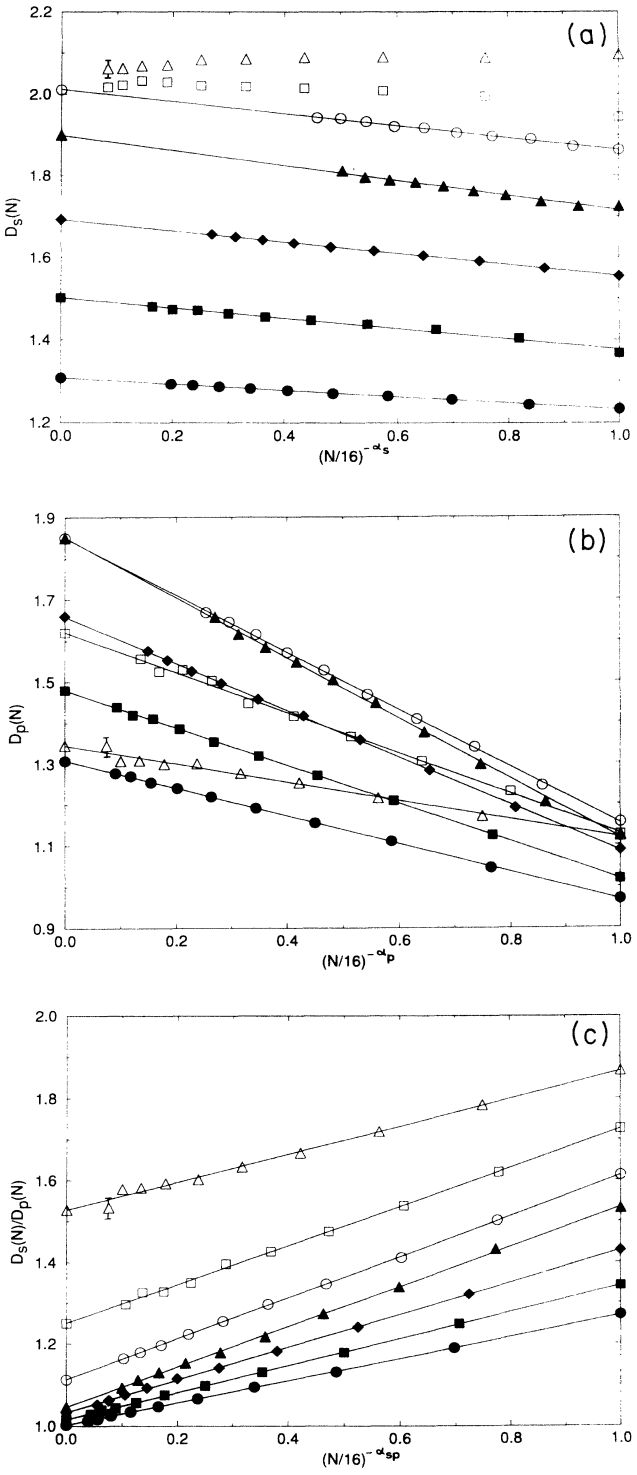

FIG. 3. Linear fits of $D_s(N)$ versus $(\frac{N}{16})^{-\alpha_s}$ (a), $D_p(N)$ versus $(\frac{N}{16})^{-\alpha_s}$ (b), and $\frac{D_s(N)}{D_p(N)}$ versus $(\frac{N}{16})^{-\alpha_{sp}}$ (c) for some D values. Filled symbols, circles, squares, diamonds and triangles, correspond to $D < 2$ values, $D = 1.3$, 1.5, 1.7, and 1.9, respectively. Open symbols circles, squares and triangles, correspond to $D > 2$ values, $D = 2.1$, 2.3, and 2.5, respectively. In each cases, the exponents α_s, α_p and α_{sp} have been chosen to give the best fit except in a) for $D = 2.3$ and $D = 2.5$ where $\alpha_s = 0.4$. The infinite-N extrapolated values are represented by the corresponding symbols on the vertical axis.

In these two cases the procedure works for all D values. The results obtained for α_s, α_p, α_{sp} and the extrapolated estimates of D_s, D_p, and $\frac{D_s}{D_p}$ are reported in Fig. 4.

The numerical errors on the parameters of the fits can be estimated as in standard regression methods. The errors on the exponents α_s, α_p, α_{sp} are quite large, of order 0.1, and are larger when D is close to 2, but it should be remembered that the presence of other terms in the large N expansion (which are not taken into account in our fits) should produce some other (systematic) errors. Our numerical results suggest that there might be an unique D-dependent α exponent in the leading correction to scaling for both $D_s(N)$ and $D_p(N)$.

In the case of D_s, the extrapolated values are almost equal, within the error bars, to the "trivial" result:

$$D_s = D \text{ for } D < 2, \quad D_s = 2 \text{ for } D > 2 . \tag{12}$$

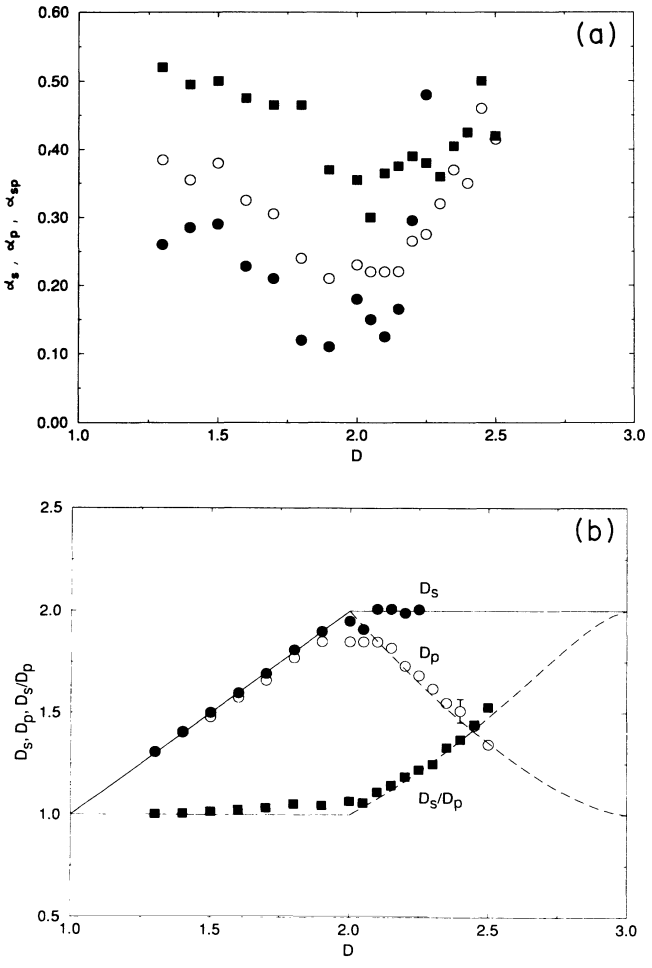

FIG. 4. The exponents α_s, α_p and α_{sp} (a) and the extrapolated values D_s, D_p and $\frac{D_s}{D_p}$ (b) as a function of D, obtained from the fits of the finite size results. Filled circles, open circles, filled squares correspond to D_s, D_p and $\frac{D_s}{D_p}$, respectively. In case (b), the solid lines correspond to the trivial results $D_s = D_p = D$ for $D < 2$ and $D_s = 2$ for $D > 2$, while the dotted lines correspond to formulae (13) and (14).

This result is consistent with the scaling $N_s \sim N^{2/D}$ for $D > 2$, which can be checked directly on our numerical results and which was already found by Meakin *et al.* [15] when analyzing the cross section of some restructured cluster-cluster aggregates scattered by ballistic point particles. Even if we cannot obtain linear fits for $D > 2.25$, the numerical results of $D_s(N)$ are consistent with an infinite-N limit of 2.

In the case of D_p, even if finite size effects are more important, the extrapolated results are consistent with the trivial result $D_p = D$ for all D smaller than 2. This means that for $D < 2$ even if there are few overlaps producing some loops, or some blobs, these overlaps are not relevant, and both the perimeter and the surface of the two-dimensional projection scale as the total mass of the three-dimensional aggregate as soon as it can be considered sufficiently large.

The new result of this work concerns D_p for $D > 2$. Here we find a nontrivial extrapolated value clearly different from both one and two and varying continuously with D. The dotted lines shown in Fig. 4(b) correspond to the following analytical expressions:

$$D_p = 1 + (3 - D)^{\frac{3}{2}} , \tag{13}$$

$$\frac{D_s}{D_p} = \frac{2}{1 + (3 - D)^{\frac{3}{2}}} . \tag{14}$$

The validity of such a formula should not be taken too seriously. It should be considered as an example of an approximate expression for D_p satisfying the boundary conditions $D_p = 2$ for $D = 2$ a nd $D_p = 1$ for $D = 3$ and going through our numerical results within the error bars.

V. CONCLUSION

The most important conclusion of this paper concerns the fractal dimension of the perimeter of the projection of a three-dimensional fractal aggregate. We have found that, in the asymptotic limit of very large aggregates, this quantity is well defined and varies continuously with the mass fractal dimension of the three-dimensional aggregate and we have been able to propose some approximate formula to account for this variation. It is therefore tempting to conclude that one might generally be able to extract the fractal dimension of a three-dimensional fractal aggregate by quantitatively analyzing the perimeter of its two-dimensional projection, even when the fractal dimension is larger than two. But before giving such a hopeful conclusion, one should investigate the degree of universality of such a result. It has been here established for a given class of "mass fractal" aggregates grown through a particular cluster-cluster algorithm. According to Ref. [12], we have strong reasons to think that our model covers a large class of experimental objects, but one should pursue and check if our results are also valid for particle-cluster aggregates (we recall that the fractal dimension of the three-dimensional Witten-Sander aggregate is equal to 2.5 [16], and therefore larger than 2). We

also intend to apply our results to an image analysis of two-dimensional photographs of carbon black aggregates. The mass fractal dimension will be estimated from the size dependence of an effective fractal dimension for the perimeter. We will also extend our numerical investigations to three-dimensional "surface fractals," i.e., compact objects bounded by a (generally self-affine) fractal surface. Here again we will try to extract their fractal properties from a quantitative analysis of their projection's perimeters.

[1] B. B. Mandelbrot, *The Fractal Geometry of Nature* (W. H. Freeman and Co., San Francisco, 1982).
[2] R. Jullien and R. Botet, *Aggregation and Fractal Aggregates* (World Scientific, Singapore, 1987).
[3] P. Meakin, Adv. Colloid Int. Sci. **28**, 249 (1988).
[4] D. Avnir, *The Fractal Approach to Heterogeneous Chemistry* (Wiley, Chichester, 1989).
[5] S. Forrest and T. Witten, J. Phys. A **12**, L109 (1979).
[6] M. Tencé, J. P. Chevalier, and R. Jullien, J. Phys. (France) **47**, 1989 (1986).
[7] F. Ehrburger-Dolle and M. Tencé, Carbon **28**, 448 (1990).
[8] D. Schaefer, J. Martin, P. Wiltzius, and D. Cannell, Phys. Rev. Lett. **52**, 2371 (1984).
[9] T. Freltoft, J. K. Kjems, and S. K. Sinha, Phys. Rev. B **33**, 269 (1986).
[10] R. Vacher, T. Woignier, J. Pelous, and E. Courtens, Phys. Rev. B **37**, 6500 (1988).
[11] M. V. Berry, J. Phys. A **12**, 781 (1979).
[12] R. Thouy and R. Jullien, J. Phys. A **9**, 2953 (1994).
[13] R. Ball and R. Jullien, J. Phys. Lett. (France) **45**, L1031 (1984).
[14] P. B. Warren, J. Phys. I (France) **3**, 1509 (1993).
[15] P. Meakin, B. Donn, and G. W. Mulholland, Langmuir **5**, 510 (1989).
[16] P. Meakin, Phys. Rev. A **33**, 3371 (1986).